

# Radiative Feedback From Runaway Massive Stars

Jonathan Mackey

Argelander-Institut für Astronomie, Universität Bonn, Germany.

Collaborators:

Dominique M.-A. Meyer,  
Vasilii V. Gvaramadze,  
Norbert Langer

see arXiv:1209.0455  
and D. Meyer's poster.

- Motivation and the example of Zeta Oph.
- 2D simulation results.
- 3D simulations (preliminary results).
- Conclusions and future work.



Unterstützt von / Supported by



**Alexander von Humboldt**  
Stiftung / Foundation

The Low-Metallicity ISM: Chemistry, Turbulence and Magnetic Fields.

Göttingen, 8-12 October, 2012.

# Introduction and Motivation

- O stars have ionising-photon energy outputs  $E > 10^{51}$  erg over their lifetimes... heating, shocks, shells.
- This is much larger than wind kinetic energy (especially at lower metallicity).
- Up to 25% of massive stars are exiled from their birthplace, as “runaways” ( $V_* > 30$  km/s) or “field stars” (Gies, 1987).
- Their feedback effects are distributed more widely through the Galaxy, esp. out of the Galactic plane.
- They explode in random places (e.g. Eldridge, Langer, & Tout, 2011).
- Are they important to ISM structure or dynamics?

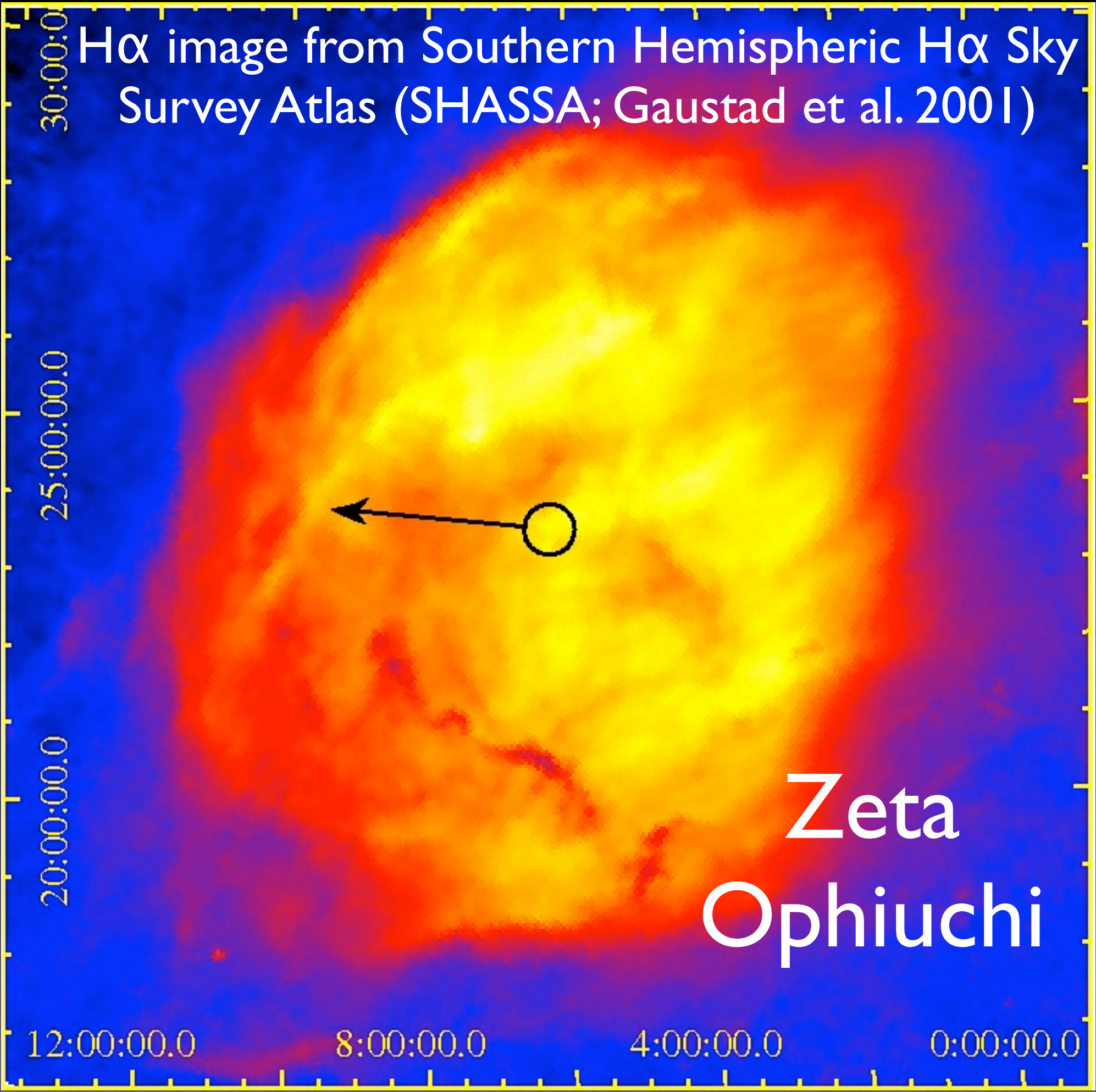
# Questions to address

- How does photoionisation affect the ISM?
- How does photoionisation affect gas dynamics within the HII region?
- How do ISM dynamics, substructure, magnetic fields affect the HII region?
- What does all this mean for the wind bow shocks?
- What can we learn about the runaway star?

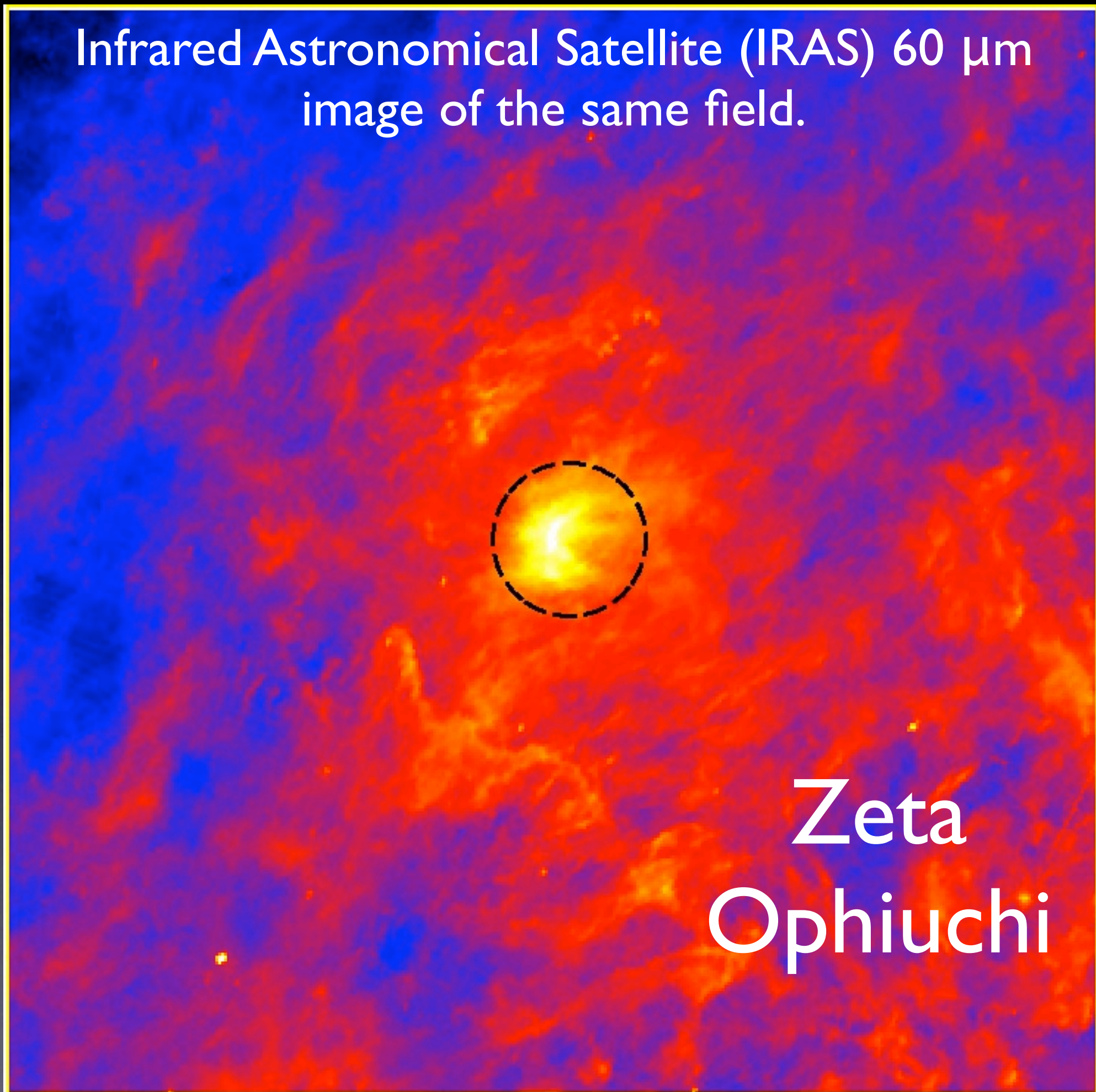
# Zeta Ophiuchi

- O 9.5Vnn runaway star (Morgan, Code & Whitford 1955).
- Distance  $d \approx 112$  pc (van Leeuwen 2007).
- Space Velocity in ISM  $v^* = 26.5$  km/s (for this distance).
- rapidly rotating ( $v \sin i = 400$  km/s, Howarth & Smith, 2001) and He enriched, so secondary of a binary system with supernova?
- Has magnetic field  $\sim 150$ G (Hubrig+, 2011, AN).
- Widely varying estimates of mass-loss rate,  $\dot{M}$ .
- $\dot{M}(\text{UV}) \approx 1.58 \times 10^{-9} M_{\odot} \text{yr}^{-1}$  (Marcolino+, 2009),  
 $\dot{M}(\text{H}\alpha) \approx 1.43 \times 10^{-7} M_{\odot} \text{yr}^{-1}$  (Mokiem+, 2005),  
 $\dot{M}(\text{theory}) \approx 1.29 \times 10^{-7} M_{\odot} \text{yr}^{-1}$  (Vink+, 2000),  
 $\dot{M}(\text{theory}) \approx 1.3 \times 10^{-8} M_{\odot} \text{yr}^{-1}$  (Lucy, 2010).

H $\alpha$  image from Southern Hemispheric H $\alpha$  Sky Survey Atlas (SHASSA; Gaustad et al. 2001)

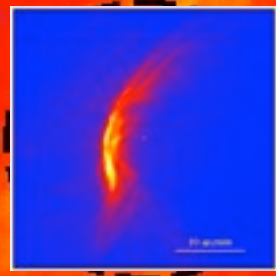


Infrared Astronomical Satellite (IRAS) 60  $\mu\text{m}$   
image of the same field.



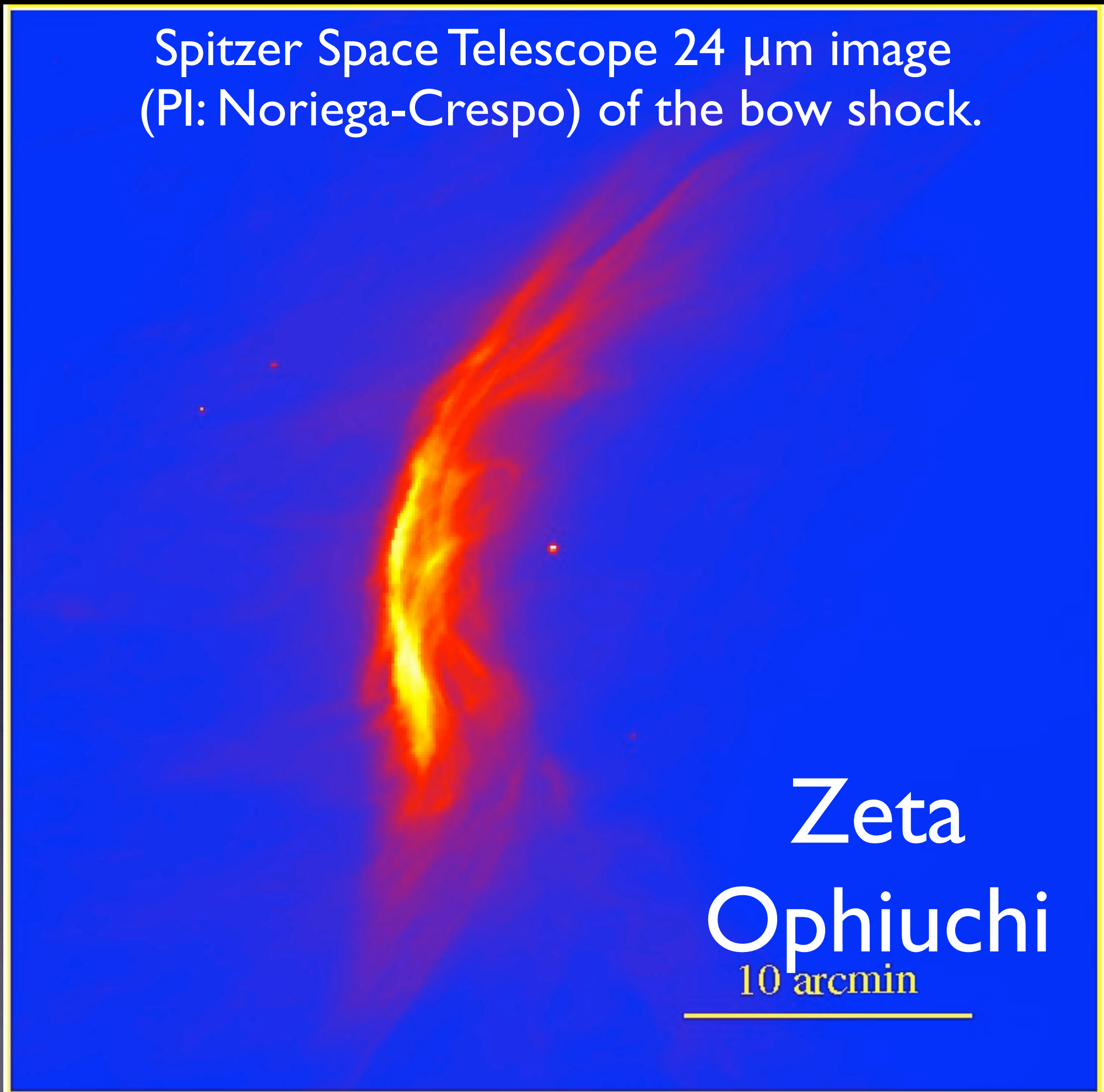
Zeta  
Ophiuchi

Infrared Astronomical Satellite (IRAS) 60  $\mu\text{m}$   
image of the same field.



Zeta  
Ophiuchi

Spitzer Space Telescope 24  $\mu\text{m}$  image  
(PI: Noriega-Crespo) of the bow shock.



Zeta

Ophiuchi

10 arcmin

---

# Constraining Mass-loss rate

Bow shock radius

$$R_0 = \left[ \frac{\dot{M} v_\infty}{4\pi n (\mu m_H v_*^2 + 2kT)} \right]^{1/2}$$

HII region radius

$$R_{St} = \left( \frac{3S(0)}{4\pi \alpha_B n^2} \right)^{1/3}$$

$$\begin{aligned} \dot{M}_{obs} v_\infty = & 1.57 \times 10^{25} \text{ g cm s}^{-2} \left( 1 + \frac{1}{M^2} \right) \left( \frac{R_0}{0.1 \text{ pc}} \right)^2 \\ & \times \left( \frac{v_*}{10 \text{ km s}^{-1}} \right)^2 \left( \frac{S(0)}{10^{48} \text{ s}^{-1}} \right)^{1/2} \left( \frac{R_{St}}{10 \text{ pc}} \right)^{-3/2}, \end{aligned}$$

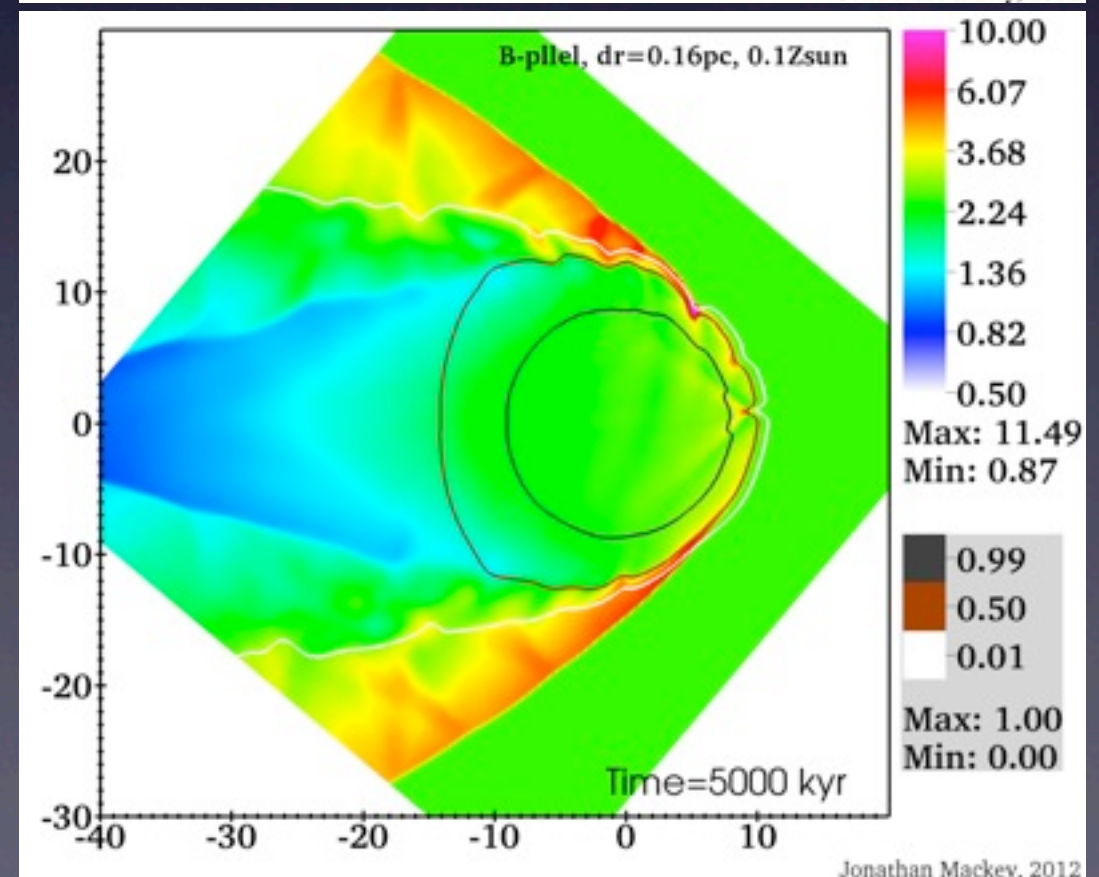
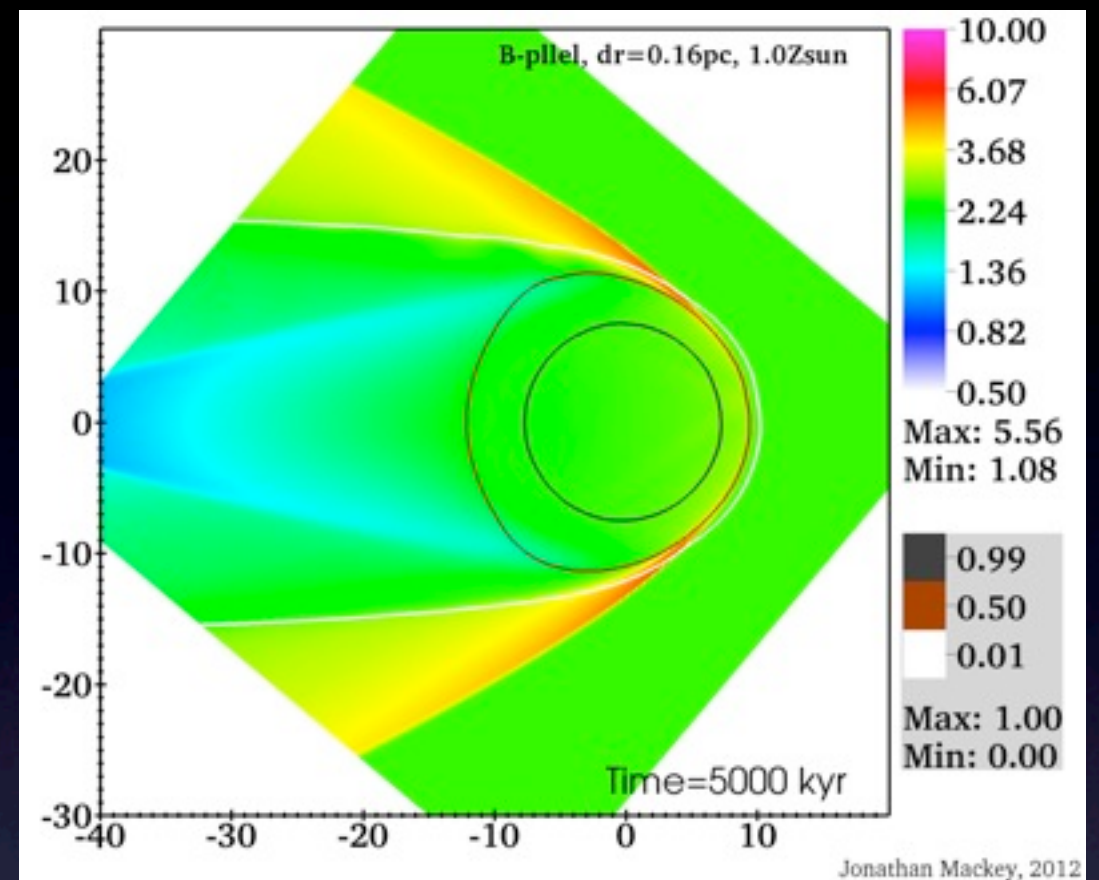
- Zeta Oph has:  $R_0=0.16 \text{ pc}$ ,  $v_*=26.5 \text{ km/s}$ ,  $R_{St} = 9.6 \text{ pc}$  (observed), and  $S(0) = 3.6 \times 10^{47} \text{ s}^{-1}$  from spectral type,  $M=2.5$  for  $T=10^4\text{K}$ .
- For  $v_\infty = 1500 \text{ km/s}$ ,  $\dot{M} = 2.2 \times 10^{-8} M_\odot \text{ yr}^{-1}$ .

# Simulations

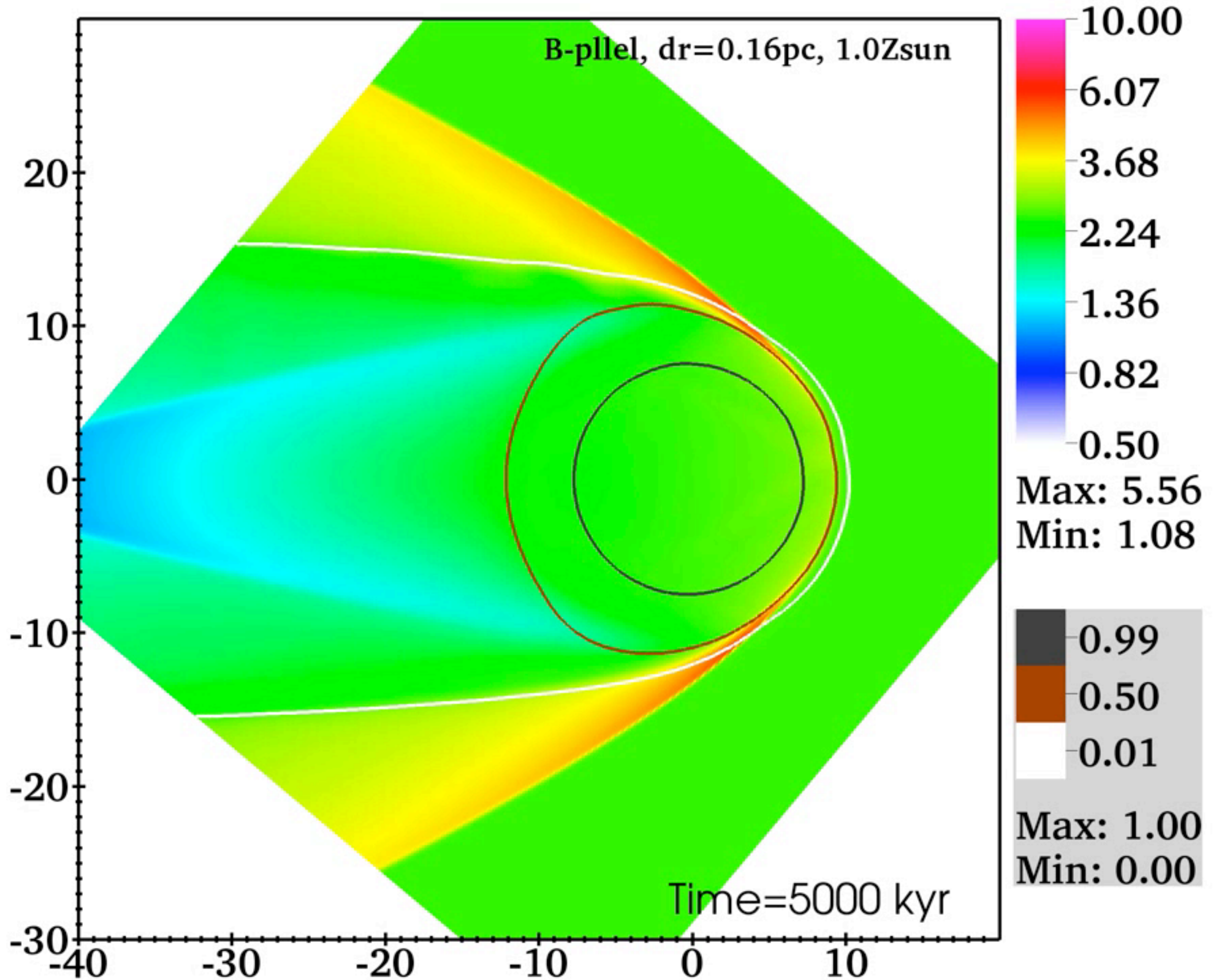
- 1D, 2D, 3D Cartesian simulations with radiation-MHD using raytracing photoionisation (Mackey+, 2010, 2011).
- Star at origin; uniform ISM flowing past star with:
  - (i) no B-field, or
  - (ii) uniform B-field with  $B \cdot v = 1$  (parallel), or
  - (iii)  $B \cdot v = 0$  (perpendicular).
- B-field strength  $7 \mu\text{G}$ . ISM density  $n_{\text{H}} = 2.5 \text{ cm}^{-3}$ .
- Neutral gas heating and cooling based on Wolfire+(2003), with metal/dust terms multiplied by a constant.
- Atomic H, He cooling calculated explicitly based on ion fraction (Frank & Mellema, 1994, Hummer 1994).
- Photoionised gas has cooling from C, O, (Henney+2009).
- <http://www.astro.uni-bonn.de/~jmackey/numerical.html>

# 2D radiation-hydro/MHD simulations

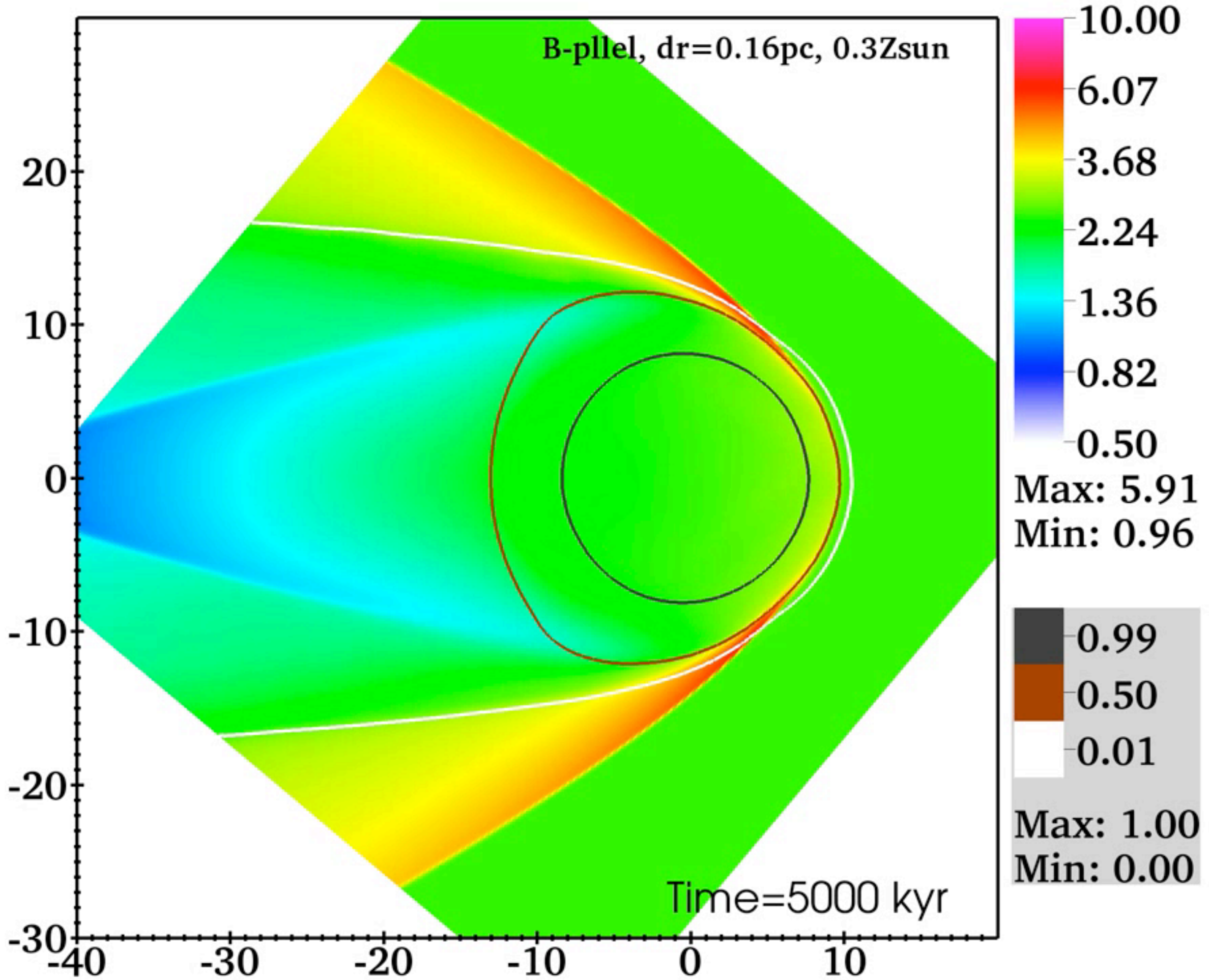
- Cartesian dynamics on a 2D plane.
- Uniform ISM advects past star (at origin) at 26.5 km/s.
- O 9.5V star in ISM:  $n=2.75 \text{ cm}^{-3}$ .
- Ionising and FUV radiation included, but no stellar wind.
- Models run with parallel and perpendicular 7 $\mu$ G B-field, and pure hydrodynamics.
- Calculated for solar metallicity, 0.3x and 0.1x solar, and metal-free.
- Hot HII region expands, creating a shell at the sides (Raga+, 1997).
- Simulations relax to a stationary state, but with instability in the ionisation front.



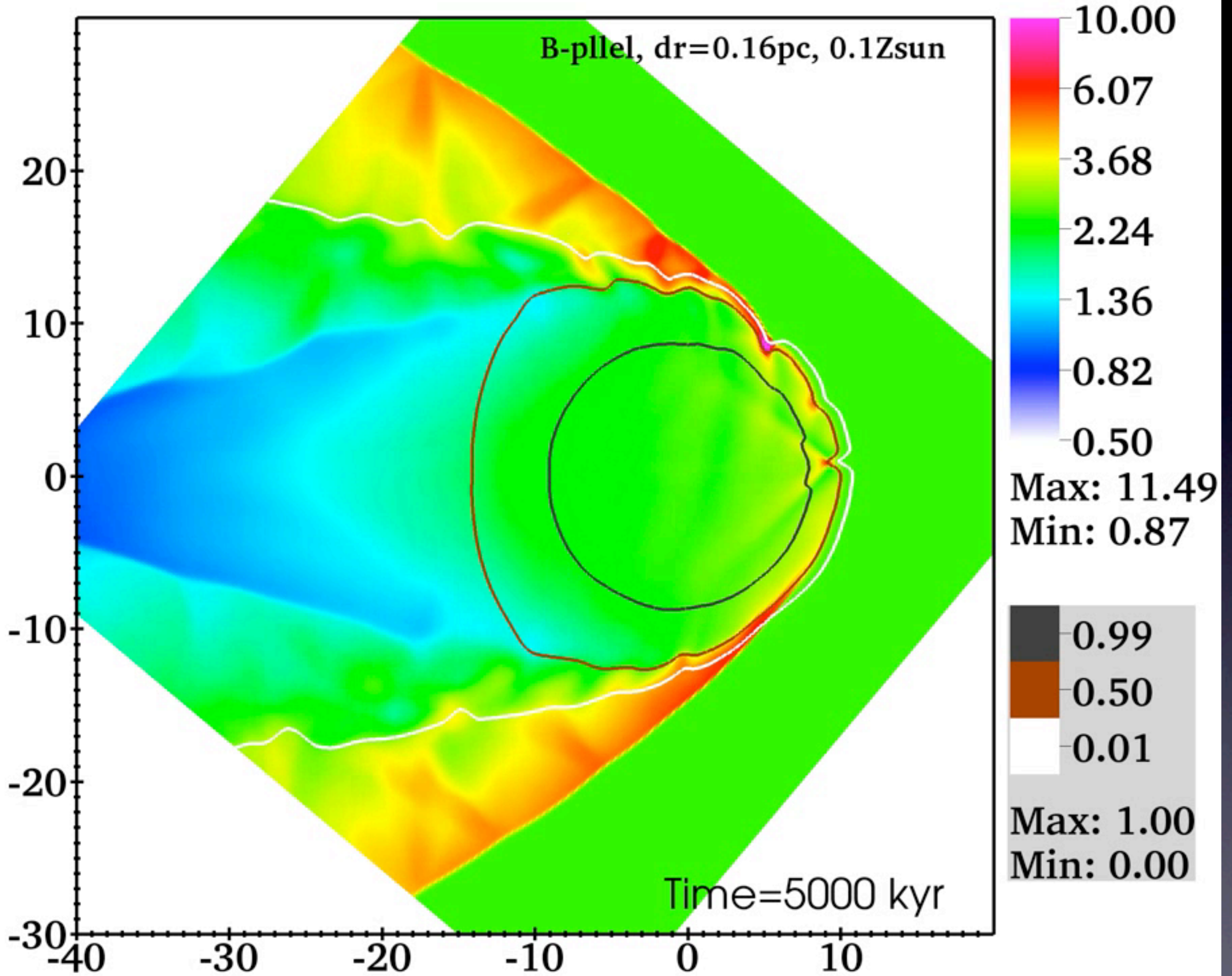




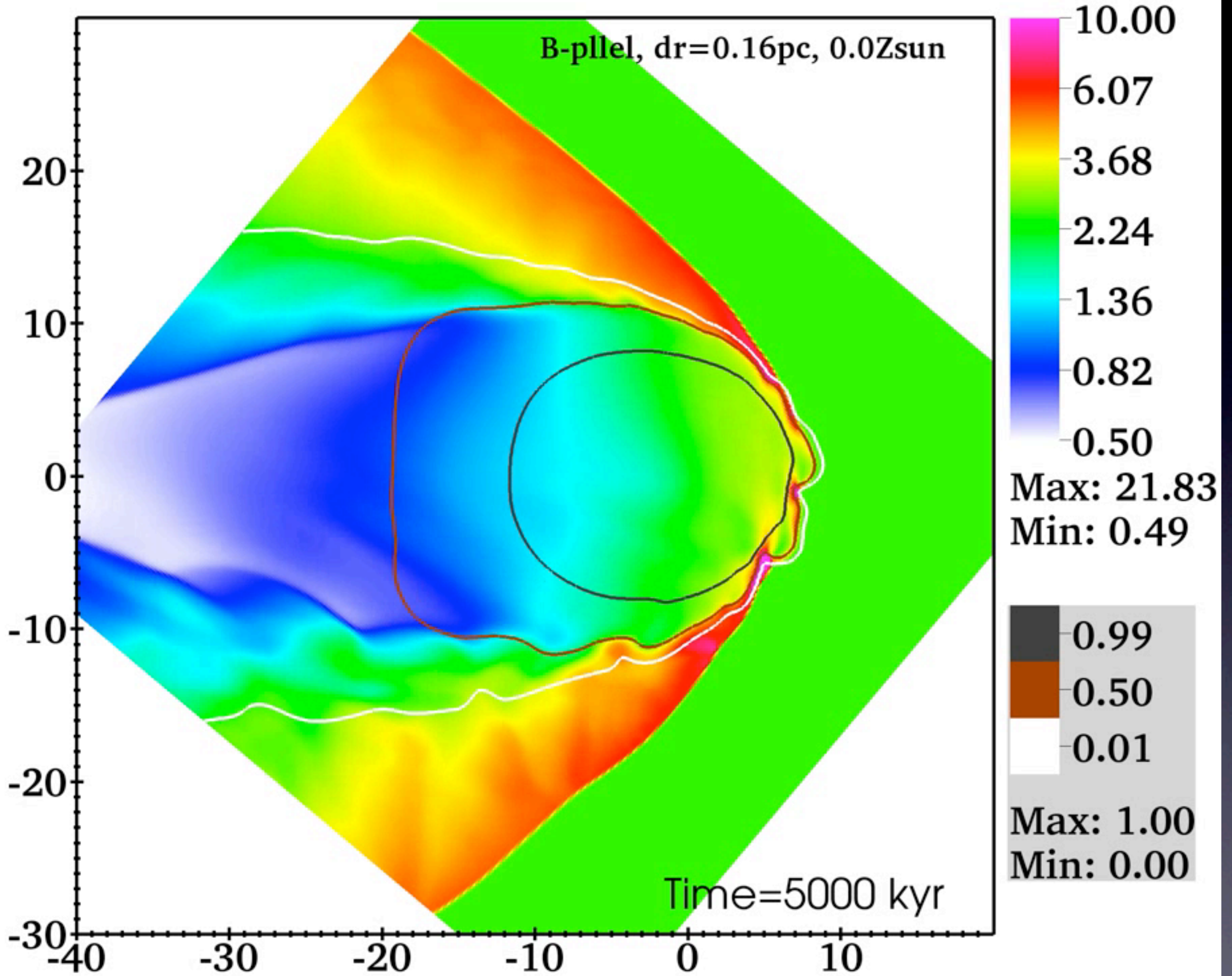




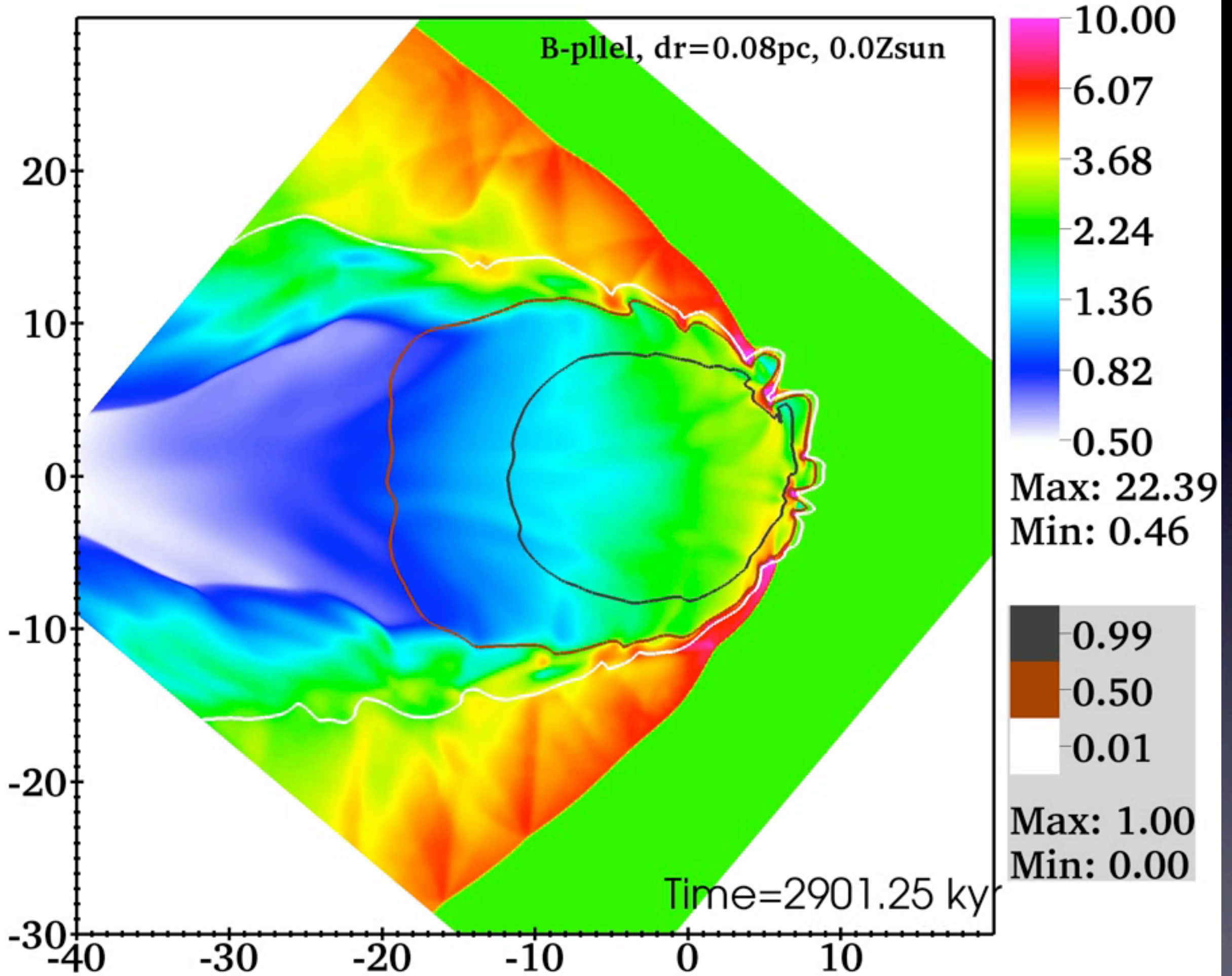




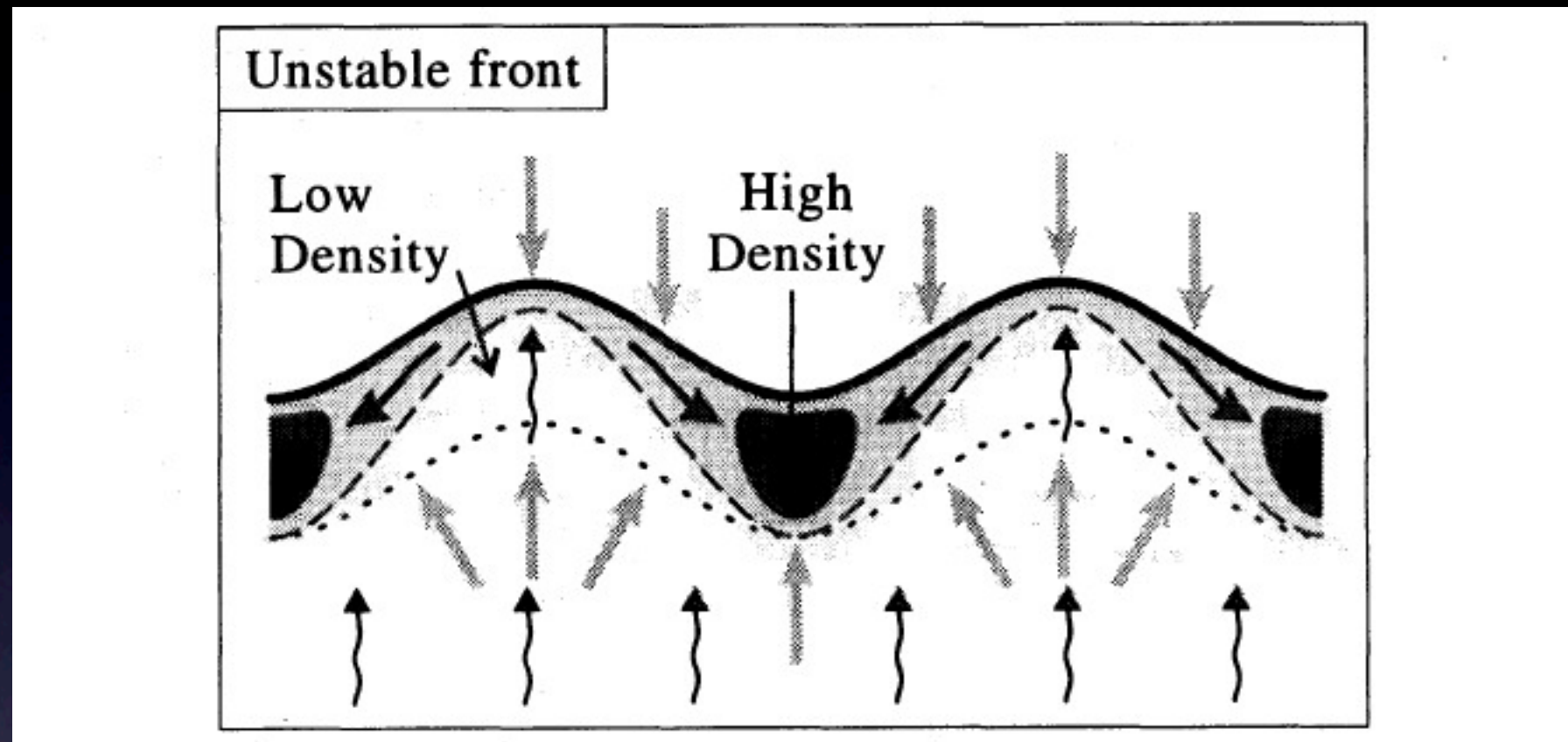








# Ionisation-front Instability



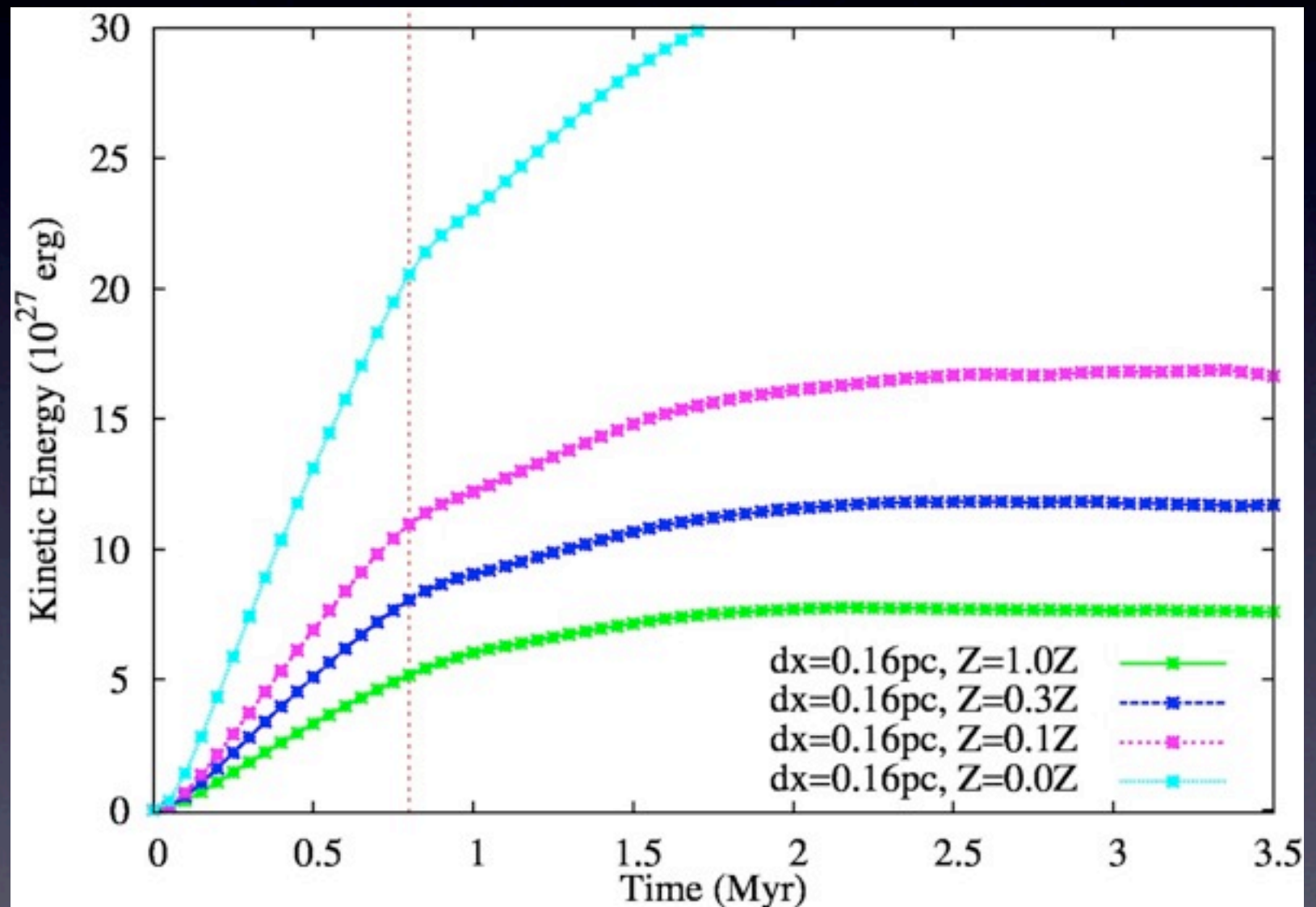
- Figure: Garcia-Segura & Franco (1996).
- We suggest that HII regions from runaway stars are the ideal place to study and observe this phenomenon.
- The ionisation front is (without instability) in steady state.
- Depending on star's velocity, can be R-type or D-type.

# A few observations

- There is an expanding conical shell of overdense gas behind star.
- Region directly behind star is underdense, moreso at lower metallicity (will be exacerbated by shocked wind).
- Ionisation front seems unstable (cf. Garcia-Segura+, 1996, Whalen & Norman, 2008), moreso at lower metallicity.
- Instability gets stronger at higher resolution.
- Gas density at star not greatly changed from ISM value.
- Conversion of thermal to kinetic energy is more efficient at low metallicity.
- 2 reasons: HII region is hotter, shocks are less dissipative.

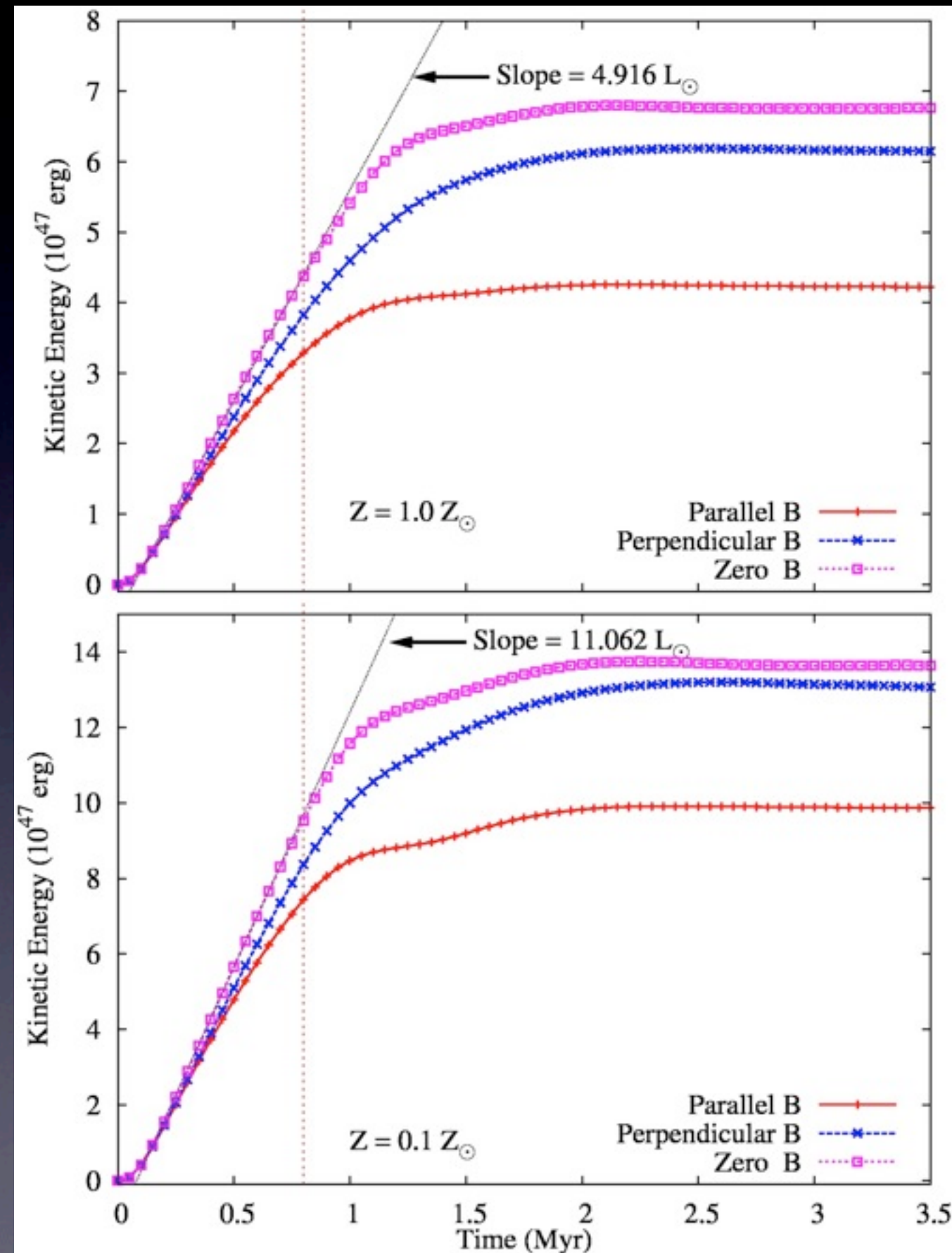
# Kinetic Energy as a function of metallicity.

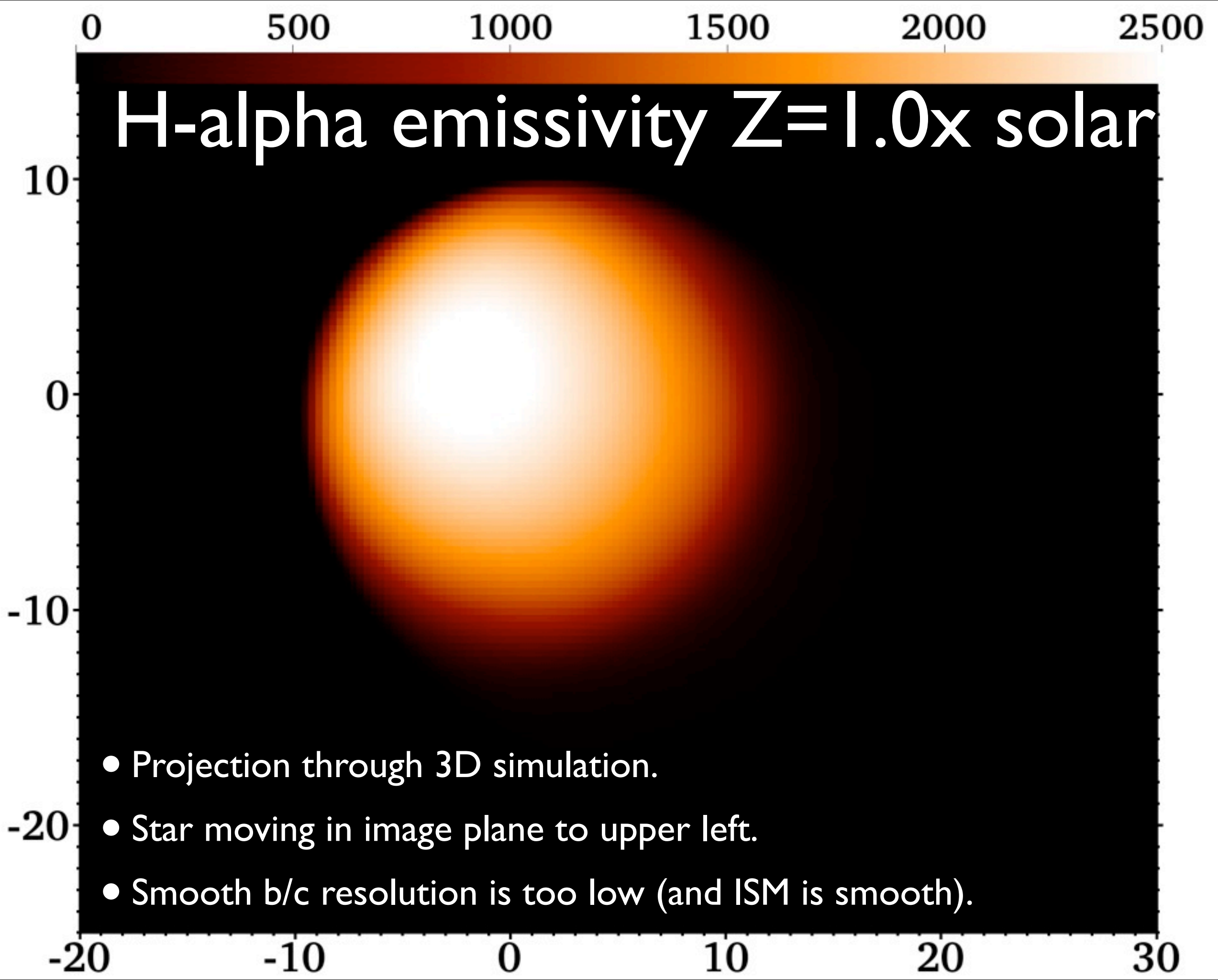
- Results shown for perpendicular B-field simulations.
- resolution  $dx=0.16\text{pc}$ .
- Steady increase of KE with decreasing metallicity.
- Reasons: hotter HII regions, less dissipation.
- HII region temperatures 6750 K, 8250 K, 9600 K, and 15000 K, respectively.
- Higher temperatures can drive stronger shocks.

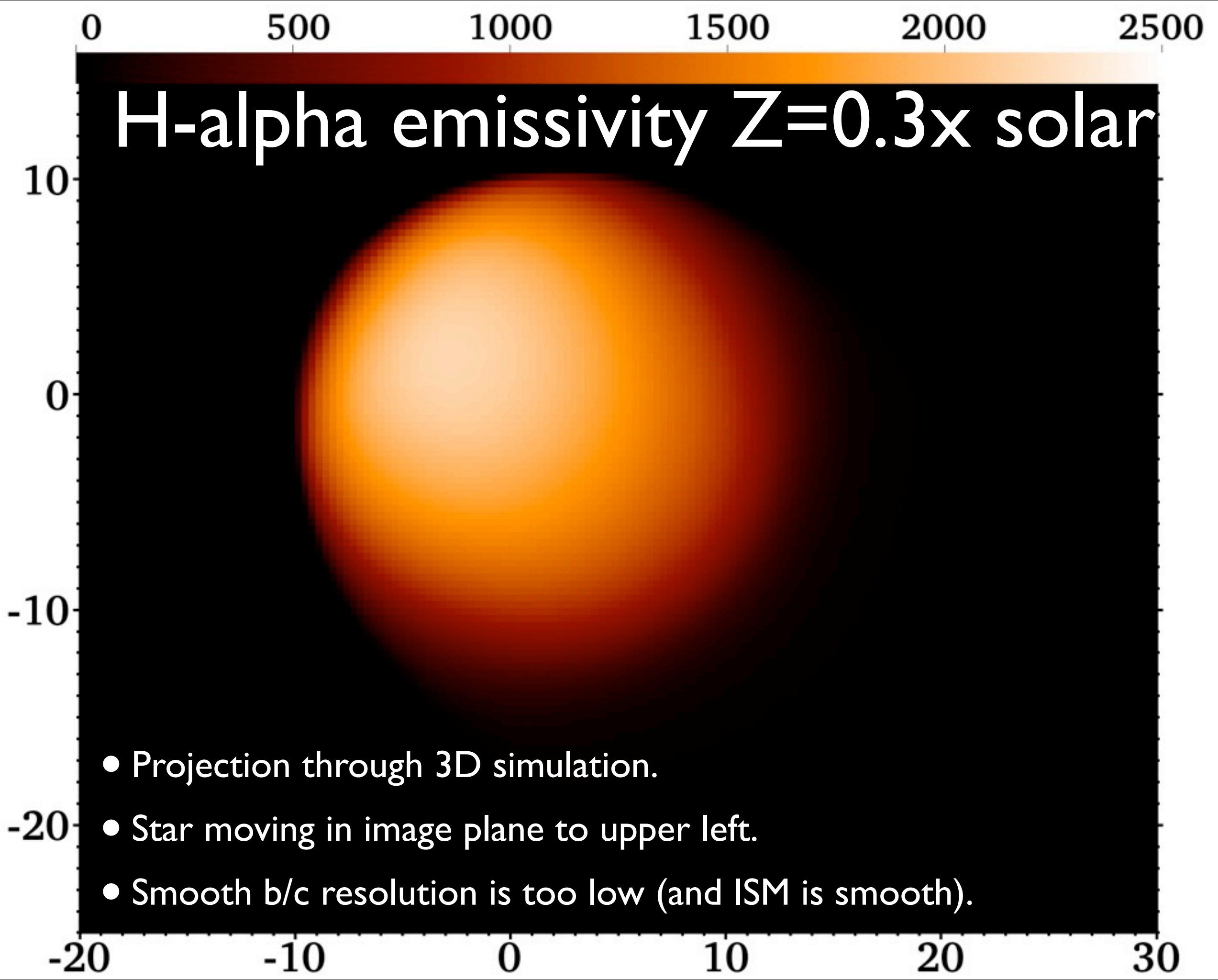


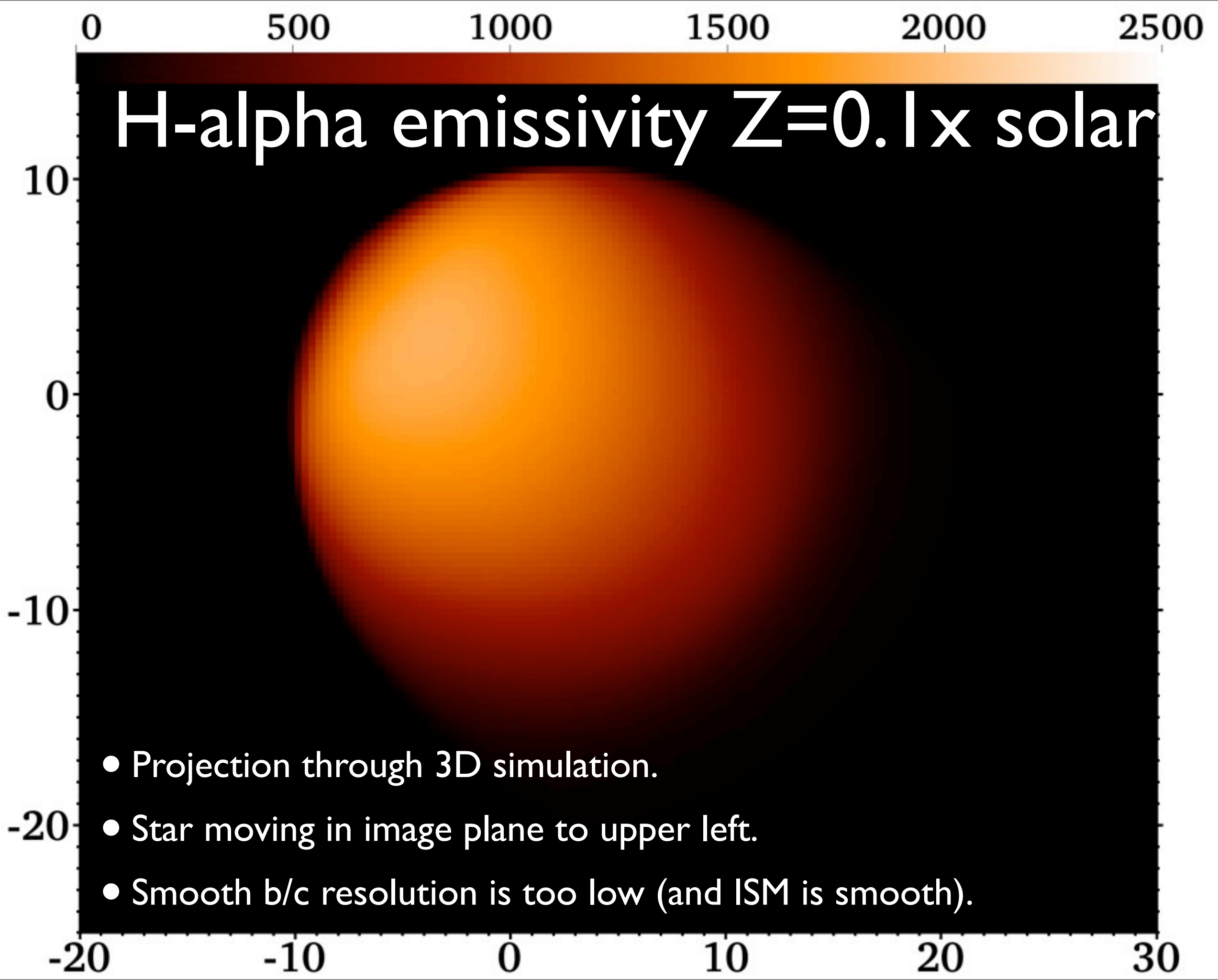
# 3D simulations (preliminary)

- Same stellar source, same velocity.
- Low resolution:  $160^3$ , with cell size  $dx=0.32\text{pc}$ .
- Insufficient to resolve I-front instability.
- Same trend is seen, of increasing kinetic energy with decreasing  $Z$ .
- Efficiency of photon-to-K.E. conversion is low (0.25% for solar metallicity,  $\sim 1\%$  for metal-free).
- Even still, K.E. of HII region shocks is larger than wind K.E. input even at solar metallicity.
- $160^3$  needs  $\sim 300$  cpu-hours,  $320^3 \sim 5000$  c.h,  $640^3 \sim 100\text{k}$  c.h.

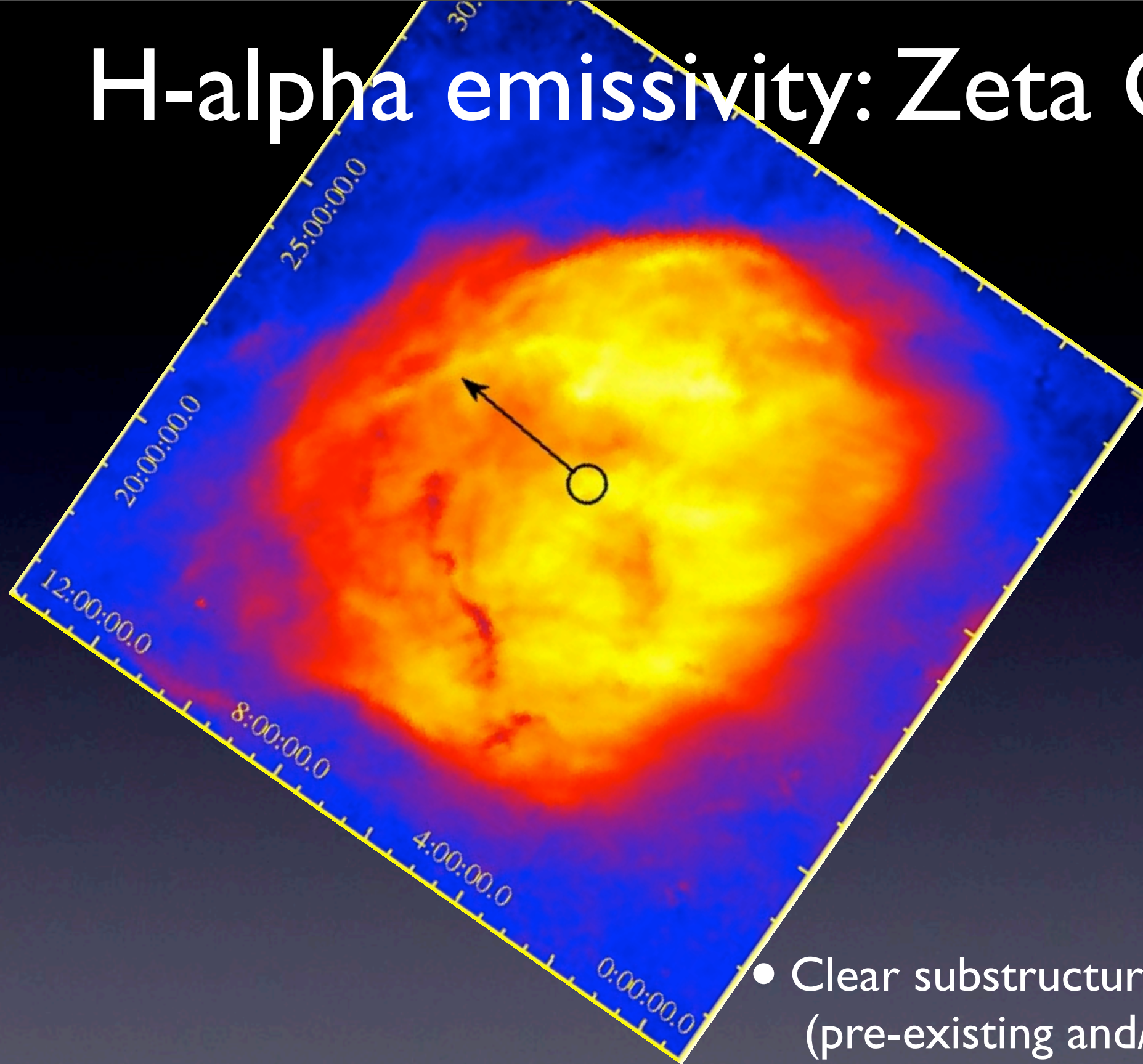








# H-alpha emissivity: Zeta Oph



- Clear substructure and clumpiness (pre-existing and/or self-generated)
- Upstream is bow-shaped, downstream is flatter.
- Modelling still needs a bit of work...

# Conclusions and Future Work

- Dynamics of HII regions around moving stars is complicated.
- Runaway stars are ideal laboratories for observing/modelling ionisation fronts.
- 2D and 3D simulations have unstable ionisation fronts, forming dense knots of neutral gas (cf. Garcia-Segura & Franco, 1996).
- Kinetic energy is inefficiently generated from ionisation heating ( $\sim 1\%$  or less), but can still be at a greater rate than wind mechanical feedback.
- Despite the unstable ionisation front:
  - Global shape and properties of HII region are not much affected.
  - ISM density at star affected only at the 10-30% level.
- Future work:
  - 3D simulations with higher resolution (in progress).
  - Modelling stellar wind bow shocks (see D. Meyer's poster!).
  - Non-uniform turbulent ISM (3D simulations cf. Mellema+, 2006).
  - Explode supernovae into the pre-computed circumstellar medium.